Arch Microbiol (2010) 192:691–702
DOI 10.1007/s00203-010-0592-6

ORIGINAL PAPER

The small RNA Aar in *Acinetobacter baylyi*: a putative regulator of amino acid metabolism

Dominik Schilling · Sven Findeiß · Andreas S. Richter · Jennifer A. Taylor · Ulrike Gerischer

Received: 6 April 2010 / Revised: 20 May 2010 / Accepted: 24 May 2010 / Published online: 18 June 2010

Abstract Small non-coding RNAs (sRNAs) are key players in prokaryotic metabolic circuits, allowing the cell to adapt to changing environmental conditions. Regulatory interference by sRNAs in cellular metabolism is often facilitated by the Sm-like protein Hfq. A search for novel sRNAs in *A. baylyi* intergenic regions was performed by a biocomputational screening. One candidate, Aar, encoded between *trpS* and *sucD* showed Hfq dependency in Northern blot analysis. Aar was expressed strongly during stationary growth phase in minimal medium; in contrast, in complex medium, strongest expression was in the exponential growth phase. Whereas over-expression of Aar in trans did not affect bacterial growth, seven mRNA targets predicted by two in silico approaches were upregulated in stationary growth phase. All seven mRNAs are involved in *A. baylyi* amino acid metabolism. A putative binding site for Lrp, the global regulator of branched-chain amino acids in *E. coli*, was observed within the *aar* gene. Both facts imply an Aar participation in amino acid metabolism.

Keywords *A. baylyi* · Hfq · IntaRNA · RNAup · sRNAs

Communicated by Wolfgang Buckel.

D. Schilling · U. Gerischer
Institute of Microbiology and Biotechnology,
University of Ulm, 89069 Ulm, Germany

S. Findeiß
Bioinformatics Group, Department of Computer Science,
Interdisciplinary Center for Bioinformatics,
University of Leipzig, 01407 Leipzig, Germany

A. S. Richter
Bioinformatics Group, Department of Computer Science,
University of Freiburg, 79110 Freiburg, Germany

J. A. Taylor
Department of Microbiology,
University of Georgia, Athens, GA 30602-2605, USA

D. Schilling (✉)
Department of Conservative Dentistry and Periodontology,
University of Ulm, Albert-Einstein-Allee 11,
89069 Ulm, Germany
e-mail: dominik.schilling@uniklinik-ulm.de

Introduction

Traditionally, RNA is thought of as ribosomal RNA (rRNA), transfer RNA (tRNA), and messenger RNA (mRNA) that function in the assembly of proteins. More than 20 years ago, the fortuitous identification of MicF RNA as a post-transcriptional regulator of mRNAs encoding outer membrane proteins changed this perception of RNA function. MicF causes translational inhibition by forming an imperfect duplex upon base-pairing with the translation-initiation region of the *trans*-encoded *ompF* mRNA (Mizuno et al. 1984; Delihas and Forst 2001; Vogel and Papenfort 2006). RNA-mediated regulation is also known to occur at the protein level. For example, 6S RNA is able to form a complex with the σ^{70} RNA polymerase holoenzyme, which leads to downregulation of σ^{70}-dependent transcription (Wassarman 2007). Another regulatory RNA, CsrB, sequesters the carbon storage regulator protein CsrA, which is a negative regulator of glycogen biosynthesis, gluconeogenesis, and glycogen catabolism, and antagonizes the CsrA ability of translation repression (Liu et al. 1997). Bacterial small regulatory RNAs (sRNAs) typically range from 50 to 250 nt in length (Hershberg et al. 2003; Altuvia 2007), with some exceptions, e.g., CsrB and RNAIII, which are 366 nt and 514 nt in length (Liu et al.

1997; Boisset et al. 2007). To detect novel bacterial sRNAs, systematic bioinformatic searches have been performed and have identified numerous sRNAs expressed within intergenic DNA regions (Argaman et al. 2001; Axmann et al. 2005; Livny et al. 2006). Whereas these bioinformatic predictions focused strictly on intergenic regions, experimental approaches have been applied to clone all RNAs of 30–65 nt or 50–500 nt and screen for novel sRNAs (Kawano et al. 2005; Willkomm et al. 2005; Sonnleitner et al. 2008). Half of all validated sRNAs to date (over 150 sRNAs) have been identified in the model organism *Escherichia coli* and in closely related pathogenic Enterobacteriaceae including *Salmonella*, *Klebsiella*, or *Yersinia* (Hershberg et al. 2003; Livny and Waldor 2007; Gardner et al. 2009). Although the majority of known sRNAs have yet to be assigned to cellular functions, some prominent examples demonstrate that sRNAs are key players in various cellular processes. During iron starvation, RyhB from *E. coli* functions in iron metabolism by downregulating genes encoding iron-containing proteins (Masse and Gottesman 2002). The *Vibrio harvey* sRNAs Qrr 1–5 affect quorum sensing by duplex formation at the ribosome-binding site of *luxR* mRNA, which encodes the master regulator of quorum-sensing genes (Tu and Bassler 2007). Several sRNAs like Spot42, SgrS, GlmY, and Z are regulators of sugar metabolism (Gorke and Vogel 2008). Furthermore, GcvB inhibits translation of seven periplasmic substrate-binding proteins of the ABC uptake system (Sharma et al. 2007).

Altering accessibility of the ribosome-binding site by sRNA–mRNA duplex formation is the predominant regulatory mechanism of sRNAs. Such interference by *trans*-encoded sRNAs is due to incomplete base pairing often stabilized by the conserved RNA chaperone Hfq, as is the case for *ompA*-MicA and *sodB*-RyhB (Moll et al. 2003; Geissmann and Touati 2004; Udekwu et al. 2005). Hfq also mediates RNA–RNA interactions by accelerating duplex formation between sRNA and mRNA (Kawamoto et al. 2006) and interferes in polyadenylation, translation, and mRNA degradation (Brescia et al. 2003; Valentin-Hansen et al. 2004; Maki et al. 2008; Regnier and Hajnsdorf 2008). In a previous study, we could show that *Acinetobacter baylyi hfq* encodes an unusual large protein compared to other Hfqs. Its absence results in severe reduction in growth and an abnormal cell phenotype of *A. baylyi*. However, despite its abnormal size, *A. baylyi hfq* is able to complement an *E. coli hfq* mutant in vivo (Schilling and Gerischer 2009). In this report, we describe Aar (*Acinetobacter* amino acid regulator), a *trans*-encoded sRNA involved in amino acid regulation in *Acinetobacter baylyi*, a Gram-negative, strictly aerobic soil bacterium (Barbe et al. 2004; Vaneechoutte et al. 2006). One of two detected Aar transcripts is affected by *hfq* deletion. We show that an increased Aar level results in upregulation of *fadA*, *ilvI*, *ppC*, *glnA*, *serC*, *leuC*, and *gcvH* mRNAs, which all function in amino acid metabolism.

Results

Prediction of small RNAs in two *Acinetobacter* species

Comparative intergenic genome analysis of *A. baylyi* ADP1 and *A. baumannii* ATCC 17978 and secondary structural stability determination with the software RNAz (Washietl et al. 2005) revealed a list of 481 thermodynamically conserved loci (RNAz mean value: −1.533 kcal/mol) that were considered to be sRNA candidates. In a Northern blot screening, 14 sRNA candidates (RNAz mean value: −3,375 kcal/mol) were tested simultaneously within pooled ADP1 RNA (Table 1). The RNA was harvested from the stationary phase of cultures grown in both minimal medium (OD_{600} = 1.8) and LB medium (OD_{600} = 1.6) as well as from the exponential growth phase of cultures grown in minimal medium (OD_{600} = 1.0) with temperature (4 or 38°C) or salt shocks (333 mM NaCl or $FeSO_4$ depletion). Signals could be detected for two new ADP1 sRNAs (data not shown). The 190-nt sRNA *aar* locus (showing an RNAz value of −3.090 kcal/mol) was predicted within the 408-nt-long intergenic region at position 2,812,240–2,812,430 of the ADP1 genome. Adjacent genes are *trpS* (105 bases upstream) encoding tryptophanyl-tRNA-synthetase II, an enzyme catalyzing the aminoacylation of $tRNA^{Trp}$ (Schimmel and Soll 1979) and *sucD* (113 bases downstream) encoding succinyl-coA-synthetase subunit α, an enzyme involved in thioesterification of succinate during the citrate cycle (Buck and Guest 1989). Using the software TransTermHp (Kingsford et al. 2007), Rho-independent termination predictions were made by adjusting the length of the termination stem between 4 and 23. One stable stem loop structure (hairpin score: −12.2 kcal/mol) was found 47 nt downstream of the *trpS* stop codon. Additionally, 48 bases upstream of the predicted sRNA Aar 3′-end, another termination structure (hairpin score: −7.4 kcal/mol) was identified (Fig. 1). According to these terminator predictions, a separate expression of Aar and *trpS* mRNA from the same DNA strand is indicated. The *sucD* orientation is opposite to that of *trpS* and *aar* and thus must be expressed separately (Fig. 1).

Small RNA Aar is encoded as an independent *Acinetobacter* gene

To characterize the expression of sRNA *aar*, mapping of the 5′ and 3′-ends by CR-RT-PCR was conducted (Forner et al. 2007). With this method, one start and one end were

Table 1 Properties of putative small RNA genes from *Acinetobacter baylyi*

Genomic location of putative sRNA	5′-upstream	3′-downstream	Predicted φ-independent termination signal next to the sRNA gene	RNAz (kcal/mol)	Experimental result
399,985–400,223	*recD* (→)	ACIAD0400 (←)	400,196–400,214 (→)	−2.750	–
402,072–402,292	*rpsO* (→)	*pnp* (→)	402,167–402,190 (→)	−3.860	+
685,911–686,054	ACIAD0697 (→)	*lysP* (←)	685,977–685,992 (←)	−3.120	–
707,132–707,407	*nrdB* (←)	*nrdA* (←)	707,419–707,443 (→)	−2.870	–
1,000,713–1,000,808	*betI* (←)	ACIAD1011 (→)	1,000,760–1,000,793 (←)	−3.450	–
1,249,605–1,249,824	*csrA* (←)	*lysC* (←)	1,249,760–1,249,793 (→)	−3.960	–
1,494,310–1,494,429	ACIAD1496 (←)	*fdxA* (←)	1,494,408–1,494,425 (→)	−4.040	–
2,199,732–2,199,863	ACIAD2226 (←)	*dctA* (←)	2,199,836–2,199,851 (→)	−3.260	–
2,308,849–2,308,996	*himD* (←)	*rpsA* (←)	2,308,909–2,308,940 (→)	−3.320	–
2,690,494–2,690,696	ACIAD2750 (←)	ACIAD2751 (←)	2,690,673–2,690,691 (→)	−3.370	–
2,812,240–2,812,430	*trpS* (→)	*sucD* (←)	2,812,382–2,812,408 (→)	−3.090	+
2,867,114–2,867,259	*lolA* (←)	*rpmA* (←)	2,867,240–2,867,254 (→)	−4.070	–
2,859,578–2,859,367	ACIAD2929 (→)	ACIAD2930 (→)	Not predictable	−3.560/−3.890	–
2,975,473–2,975,690	ACIAD3045 (←)	*rplT* (←)	2,975,654–2,975,671 (→)	−3.640	–

Arrows indicate the orientation of the sRNA gene (according to the prediction of φ-independent termination signals) and the orientation of the respective neighbor genes. RNAz values are corresponding to the predicted φ-independent terminator. +/−: Result of Northern blot detection of the predicted sRNA

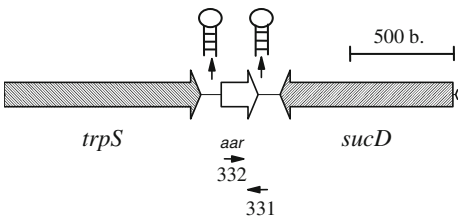

Fig. 1 Schematic drawing of the *A. baylyi aar* genomic localization. Rho-independent termination signals for *trpS* and *aar* are indicated with stem loop structures. *Numbers* and *arrows* show the annealing sites and orientation of Northern blot primers for Aar detection

mapped for *aar* to genomic positions 2,812,231 and 2,812,412, 9 nt upstream of the corresponding predicted *aar* gene start and 18 nt upstream of its end, respectively (Fig. 2a). The *aar* sequence with an AT content of almost 70% complicated the choice for CR-RT-PCR primers. Selected primers were situated at position 2,812,298–2,812,273 and 2,812,338–2,812,362 with a 40-base gap (Fig. 2c), thus perhaps preventing a successful PCR of processed transcripts. However, 5′-RACE experiments with alternative primers, annealing at position 2,812,355–2,812,335 and 2,812,319–2,812,300, detected no alternative promoter as well. These results confirm that *aar* is expressed as an independent gene rather than a polycistronic transcript with *trpS* or *sucD* (*aar* alone = 181 nt vs. *trpS-aar* = 1,194 nt or *sucD-aar* = 1,072 nt, Fig. 1).

The mapped 3′-end aligns with the predicted Aar Rho-independent transcription termination stem (2,812,382–2,812,408). Putative elements of a σ^{70} promoter with a perfect Pribnow box containing the consensus sequence TATAAT and a 50% match to the σ^{70} −35 consensus region were found upstream of the *aar* transcription start site (Fig. 2a). BLASTN analysis was performed with the mapped *aar* sequence of *A. baylyi* ADP1 and the NCBI database (nucleotide collection). *Aar* homologs were found only in *Acinetobacter baumannii* strains SDF, AB307-0294, AB0057, ACICU, AYE, and ATCC17978 with sequence identities between 69 and 71% and a 92% query coverage (missing the first nine and last five bases of ADP1 *aar*). These findings indicated that Aar is unique to *Acinetobacter*. A multiple sequence alignment with all *Acinetobacter aar* homologs is shown in Fig. 2b. While the *Acinetobacter baumannii aar* sequences share an identity of 98%, *A. baylyi* ADP1 *aar* showed only a strictly conserved 3′-end compared to the respective *A. baumannii* homologs (Fig. 2b). The genomic localization of *aar* was found to be conserved as well. At least either *trpS* or *sucD* is encoded at a position flanking the *A. baumannii aar* homologs (i.e., *A. baumannii* SDF *aar* location: upstream of *sucD* on the negative strand; *A. baumannii* AB307-0294 *aar* location: downstream of *trpS* on the same strand; *A. baumannii* ACICU *aar* location: between *trpS* and *sucD*).

Expression profile of *aar*

An Aar expression profile was created by Northern blot analysis of expression levels in *A. baylyi* ADP1 grown in minimal medium supplemented with different carbon sources (succinate or quinate) or in LB medium; RNA was collected from cells in different growth phases (early

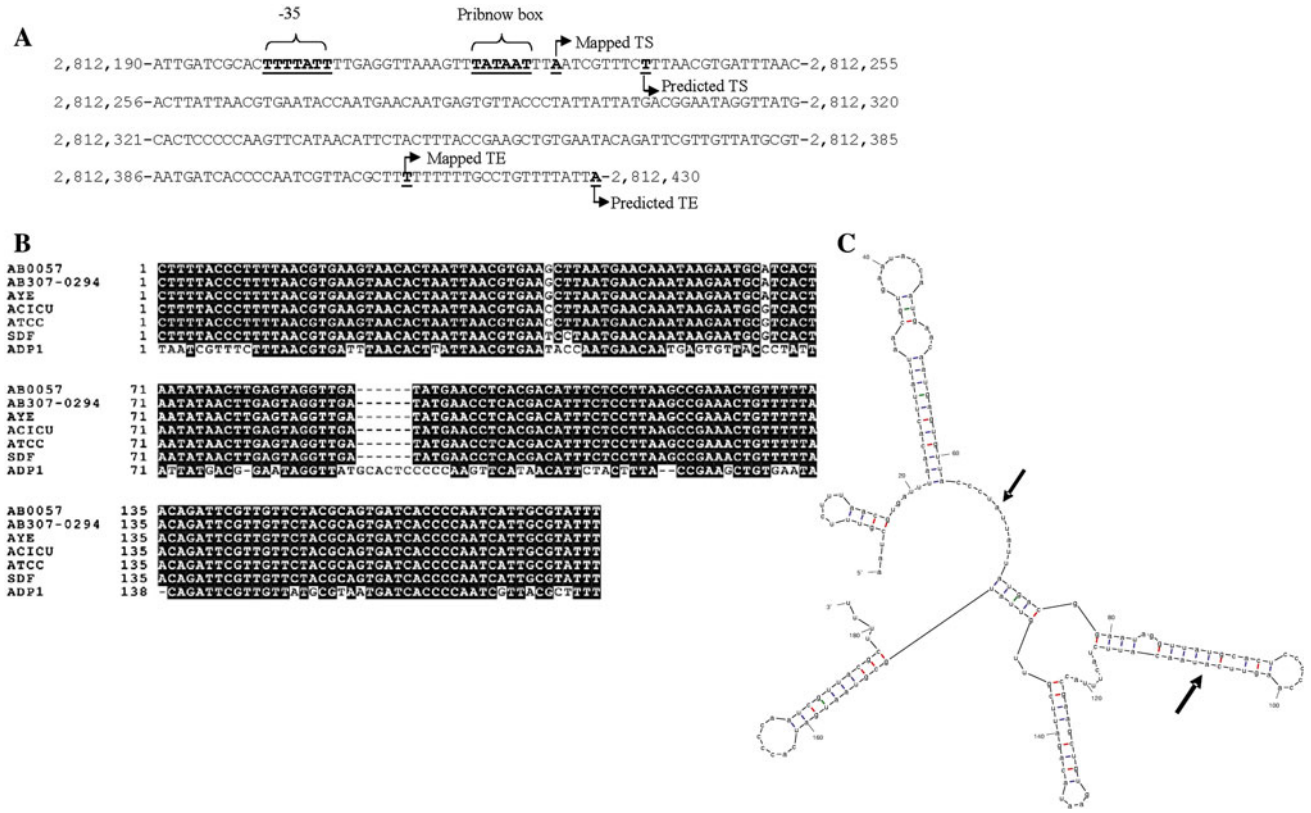

Fig. 2 Combined sequence and structure information of *A. baylyi* ADP1 Aar. **a** 5′-upstream sequence and sequence of the complete *aar* gene locus (indicated by the ADP1 genome position). *Arrows* assign the predicted (RNAz) and mapped (CR-RT-PCR) gene starts. *Highlighted in bold* Putative −10 and −35 boxes found within the promoter region of *aar* and transcription start (TS) and end (TE) sites. **b** Primary sequence alignment of *A. baylyi* ADP1 Aar with six *A. baumannii* Aar homologs (strains AB0057, AB307-0294, AYE, ACICU, ATCC 17978, SDF) calculated and visualized by ClustalW2 and BoxShade3.2, respectively. *Letters drawn in black* are conserved at least in 50% of all sequences. **c** Predicted secondary structure of *A. baylyi* ADP1 Aar calculated and visualized by Mfold. *Arrows* indicate a putative region of Aar processing

exponential [$OD_{600} = 0.4$], exponential [$OD_{600} = 1.0$], and stationary [$OD_{600} = 1.8$, minimal medium or $OD_{600} = 1.6$, LB medium]) of all these cultures. Additionally, the effects of salt shock (NaCl addition, $c_{final} =$ 333 mM), iron depletion, and temperature shocks (4 or 38°C) on Aar expression of ADP1 grown in minimal medium supplemented with succinate were determined. Furthermore, Aar expression was detected at different growth phases of a Δ*hfq* mutant and an over-expression mutant encoding *hfq* on plasmid pRK415 grown in minimal medium with succinate. Two bands were observed for the wild type and the *hfq* over-expression mutant, while only a single band was present in the Δ*hfq* mutant. Two strong signals were seen in stationary phase cells of ADP1 grown with succinate (Fig. 3 lane 3) and quinate (Fig. 3 lane 12). After cultivation of ADP1 in LB complex medium, expression was visible during exponential growth as two strong signals (Fig. 3 lane 8). The variation in the growth temperature (reduction to 4°C or ascent to 38°C) led to some negative impact on the growth rates of these cultures following the shock, but all cultures recovered and reached the same final OD_{600} (1.8) as APD1 grown under the same conditions but without shock (data not shown). Whereas the temperature changes showed no effects on Aar, an excess of sodium chloride led to early expression of Aar (Fig. 3 lanes 4–6 compared to lane 2). The effect of iron limitation was even more drastic (Fig. 3 lanes 13–14 compared to lanes 1–2). In strain *A. baylyi* pRK415 *hfq* also grown in minimal medium with succinate, Aar expression was also strong in the stationary phase (Fig. 3 lanes 15–17). Strong Aar expression in strain *A. baylyi* Δ*hfq* was seen at both growth phases checked (Fig. 3 lanes 18–19). Of special interest is the fact that the second, smaller signal is absent in the Δ*hfq* mutant. This observation may indicate that Hfq is involved—directly or indirectly—in processing of Aar.

Effects of Aar modification

A muliplex PCR strategy was kindly applied by Véronique de Berardinis to delete the *A. baylyi aar* gene. This strategy had been applied in a large number of cases to delete genes

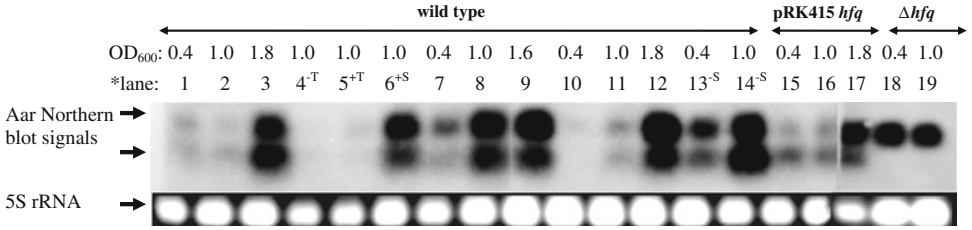

Fig. 3 Northern blot signals of Aar expressed under different conditions in three *A. baylyi* strains (ADP1 wild type, pRK415 *hfq* and Δ*hfq*). Detected 5S rRNA signals after RNA separation are illustrated under the corresponding Northern blot signals of Aar, indicating equal RNA amounts applied in each fraction. The corresponding OD_{600} value is indicated above the lanes. *Numbers* refer to growth phases and conditions for Aar detection. *Carbon sources/growth conditions: 1–6 = minimal medium (succinate); 7–9 complex medium; 10–12 = minimal medium (quinate); 13–19 minimal medium (succinate); −T = 4°C, +T = 38°C, +S = NaCl (333 mM), −S = $FeSO_4$ depletion

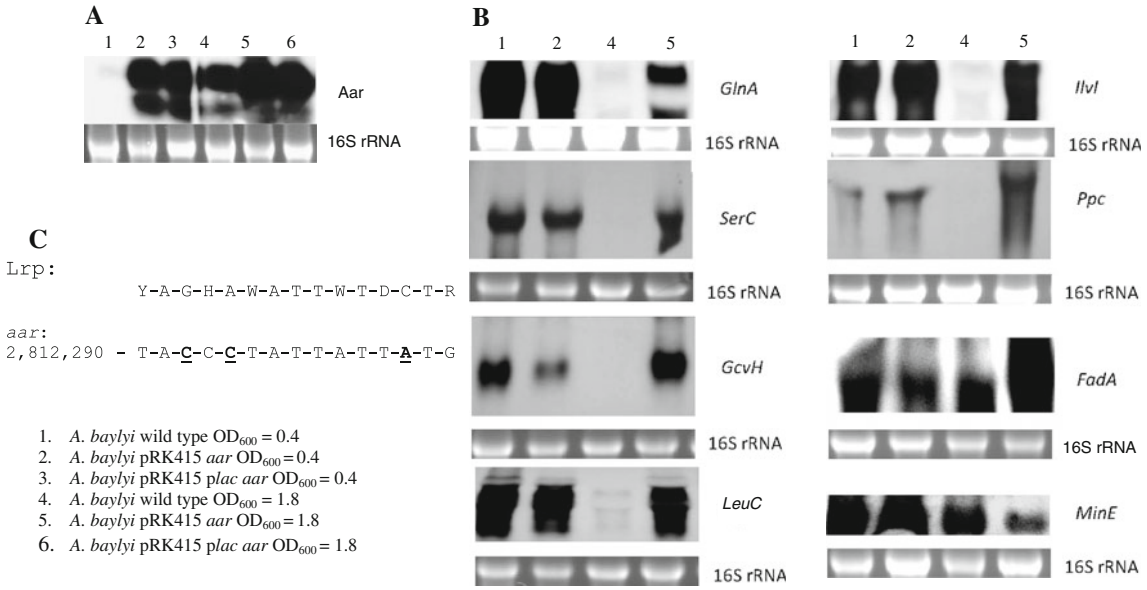

Fig. 4 Influence of Aar over-expression. **a** Detection of Aar in *A. baylyi* wild type, *A. baylyi* pRK415 *aar*, and *A. baylyi* pRK415 p*lac aar* mutants with Northern blot experiments. **b** Comparative Northern blot experiments of seven Aar–mRNA interaction partners in minimal medium with succinate (except for *fadA* mRNA: protocatechuate). Detected 16S rRNA signals after RNA separation are illustrated under the corresponding Northern blot signals, indicating equal RNA amounts applied in each fraction. *Numbers* correspond to the used *A. baylyi* strain and growth phase for RNA detection. **c** Comparison of the *E. coli* Lrp-binding site to a putative Lrp-binding site in *A. baylyi aar*. Mismatches to the *E. coli* Lrp consensus motif are indicated by ***bold underlined*** characters. Amino acid abbreviations: Y = C or T, H = not G, W = A or T, D = not C, R = A or G

in *A. baylyi* successfully (de Berardinis et al. 2008). The fact that the *aar* mutant could not be retrieved despite three attempts is a strong indication that this gene is essential. Furthermore, the impact on bacterial growth of over-expressing Aar was analyzed. Strains designed to express higher amounts of Aar were created by directional cloning of the *aar* gene into pRK415. Depending on the cloning procedure, expression of *aar* was either controlled by its own promoter (*A. baylyi* pRK415 *aar*) or by the *lac* promoter (*A. baylyi* pRK415 p*lac aar*). Aar Northern blot analysis confirmed that over-expression of Aar was successful in *A. baylyi* pRK415 *aar* as well as in *A. baylyi* pRK415 p*lac aar* with no obvious difference in the amount of Aar (Fig. 4a). These strains were tested in growth experiments in LB medium or in minimal medium with succinate, pyruvate or protocatechuate as the sole carbon source. No obvious difference was detectable in the growth behavior of these strains (data not shown). The missing phenotypes of these strains may result from the low copy number of pRK415 in *A. baylyi* (Trautwein and Gerischer 2001).

Prediction of putative Aar targets

In order to find putative mRNA interaction partners of sRNA Aar, two *in silico* predictions were performed with the programs IntaRNA (Busch et al. 2008) and RNAup (Mückstein et al. 2006). Several criteria were included in

Table 2 Predicted Aar–mRNA targets that have been selected for further experimental analysis

Gene	Function	Interaction site mRNA (relative to AUG)[a]	Interaction site Aar	Interaction energy (kcal/mol)	Prediction method	Experimental result
ppc	Pyruvate metabolism	(−11, −4)	(5, 12)	−3.79	IntaRNA	+
		(−88, −78)	(170, 180)	−7.3	RNAup	
ilvI	Branch-chained amino acid synthesis	(−14, 5)	(10, 30)	−9.08	IntaRNA	+
fadA	Branch-chained amino acid degradation	(−18, −8)	(5, 15)	−9.91	IntaRNA	+
serC	Serine synthesis	(−12, −2)	(2, 12)	−8.05	IntaRNA	+
leuC	Branch-chained amino acid synthesis	(−10, −1)	(144, 153)	−2.88	IntaRNA	+
glnA	Nitrogen fixation into glutamine	(−14, −7)	(43, 50)	−5.46	IntaRNA	+
glnT		(15, 27)	(4, 16)	−4.17	IntaRNA	n.d.[b]
minE	Cell division	(−28, 34)	(117, 170)	−5.92	IntaRNA	−
gcvH	Glycine degradation	(−28, 49)	(161, 181)	−6.72	RNAup	+
		(−16, −6)	(7, 17)	−5.3	IntaRNA	

[a] IntaRNA predictions were filtered to cover the ribosomal-binding site. Therefore, the interaction sites are close to the start codon AUG

[b] mRNA not detected

RNAup predictions were filtered by conservation of the sRNA–mRNA interaction. Thus, the resulting interaction sites are widely spread across the mRNA

+/− corresponds to an observed influence on mRNA level upon Aar over-expression or not

both predictions to constrain putative interaction partners. Since the experimentally validated target sites of most sRNAs are located around the Shine Dalgarno sequence, we searched for interactions in this region. Furthermore, conserved interactions were predicted. Therefore, in the IntaRNA approach, a seed region of eight contiguous base pair interactions with conserved Aar regions (Fig. 2b bases 10–53 and 136–149) was assumed. Instead, in the RNAup approach, conserved interactions were predicted, appearing at least in 70% of the seven *Acinetobacter* strains containing *aar* homologs. From the total number of 866 putative targets of both predictions, 9 genes with good interaction energy values (mean energy value of all interactions: −3.72 kcal/mol, energy values of selected targets: Table 2) were selected for experimental analysis. Additionally, all the selected putative targets are members in regulation of amino acid biosynthesis and degradation except for *minE*. This gene encodes a cell division factor involved in FtsZ ring formation during cell division (de Boer et al. 1989). But the predicted interaction of *minE* mRNA with Aar exhibited a high energy value (−5.92 kcal/mol). Relative quantification of mRNAs of these genes was determined by comparative Northern blot experiments with total RNA from ADP1 and strain pRK415 *aar* grown in minimal medium with succinate (or protocatechuate in the case of *fadA* mRNA detection). Thereby, effects of Aar over-expression on the amount of the putative target mRNAs were studied. While *minE* mRNA levels were slightly affected by over-expression of Aar, *glnT* mRNA could not be detected. All other mRNA targets involved in amino acid metabolism were upregulated in *A. baylyi* pRK415 *aar* during stationary but not exponential growth (Fig. 4b).

Possible involvement of Lrp

Gene expression of many sRNAs is regulated by specific transcriptional regulators like Fur-RyhB, SgrR-SgrS, or LuxO-Qrr1-5 (Bejerano-Sagie and Xavier 2007; Masse et al. 2007; Vanderpool 2007). To find potential regulator-binding sites, we checked the *A. baylyi aar* gene (position 2,812,231–2,812,412) with the Prokaryotic Database of Gene Regulation PRODORIC (Munch et al. 2003). Within the *aar* sequence, 59 bases downstream of the transcription start site (position 2,812,290), we found an 80% sequence match to a confirmed 15-base pair-long binding site for the leucine-responsive protein (Lrp, Fig. 4c). Lrp is a global regulator of operons involved in amino acid biosynthesis and degradation (Calvo and Matthews 1994; Cui et al. 1995). The presence of the putative Lrp-binding site within *aar* and the accumulation of a set of mRNAs related to amino acid metabolism upon Aar over-expression might indicate that these metabolically related genes are regulated by a common mechanism, which might include the known global regulator Lrp and the newly discovered sRNA Aar.

Discussion

In this study, we report the discovery of Aar (*Acinetobacter* amino acid regulator), the first sRNA of the genus *Acinetobacter* with no homology to already known prokaryotic sRNAs. Aar was predicted by an *in silico* approach, and BLASTN analysis indicated that Aar is present only within the genus *Acinetobacter*. Within these species, the *aar*

genomic location is conserved. A few examples of species-specific sRNAs like Aar are known, including Qrr 1–5 in *Vibrio harvey* and *V. cholerae* (Bejerano-Sagie and Xavier 2007) and InvR in *Salmonella typhimurium* and *S. bongori* (Pfeiffer et al. 2007).

The size of ADP1 Aar was determined to be 181 bases, but the presence of two bands in Northern blot analysis indicates that this sRNA is processed after transcription or an alternative promoter might exist. The absence of the second, smaller Northern blot signal in the Δ*hfq* mutant suggests that Hfq, as global RNA chaperone, may play a role in Aar processing. However, recent results indicate that Hfq affects also the transcription efficiency in addition to mRNA degradation (Le Derout et al. 2010), but neither CR-RT-PCR—nor 5′-RACE—experiments detected different *aar*-promoters that would explain the absence of the smaller Aar transcript in the Δ*hfq* mutant. Thus, instead of an Hfq impact upon *aar* transcription, it is more likely that Hfq—directly or indirectly—affects Aar stability. In general, Hfq is essential for processing, polyadenylation, and degradation of RNAs (Hajnsdorf and Regnier 2000; Le Derout et al. 2003; Masse et al. 2003; Valentin-Hansen et al. 2004; Folichon et al. 2005). Furthermore, Hfq is involved in sRNA-dependent mRNA inactivation by promoting RNA structure refolding (Brescia et al. 2003; Geissmann and Touati 2004). Thereby, the Hfq interference often causes repression of mRNA translation and coupled sRNA and mRNA degradation by ribonucleases (Masse et al. 2003; Udekwu et al. 2005; Kawamoto et al. 2006). Thus, it is conceivable that the loss of Hfq may result in the accumulation of unprocessed Aar transcripts, which was seen in the Northern blot experiments with the *A. baylyi* Δ*hfq* mutant.

Under normal conditions, Aar is present in high amounts during stationary growth, which coincides with the fact that many sRNAs are induced under stress or when nutrients become scarce. For example, sRNAs identified in *E. coli* that are induced after environmental changes are RyhB under iron depletion, OxyS after oxidative stress, DsrA at low temperatures, and SgrS after the accumulation of glucose-P (Gottesman 2005). Interestingly, Aar is influenced by changing salt conditions but not by the temperature variations tested. Sodium chloride excess as well as iron depletion resulted in earlier expression of Aar during growth.

As seen by Northern blot analysis, Aar over-expression led to the accumulation of seven mRNAs that encode proteins involved in amino acid metabolism. Of these, *glnA* encodes glutamine synthetase, which assimilates nitrogen by converting glutamate and nitrogen into glutamine (Calvo and Matthews 1994). In the Aar over-expression mutant, *glnA* mRNA accumulated during stationary growth in minimal medium but the mRNA was barely detectable under normal Aar expression conditions. No differences were seen during exponential growth. Aar also affected the mRNAs *leuC*, *serC*, *ilvI*, *ppc*, *gcvH*, and *fadA* similarly.

In analogy to the DsrA–*rpoS* base pairing interaction in *E. coli* (Soper and Woodson 2008), binding of Aar far upstream of the start codon could result in opening an inhibitory secondary structure at the ribosome-binding site and thereby increasing the mRNA stability. However, the predicted Aar–mRNA interactions showed rather a sequestering than liberating potential toward the Shine Dalgarno sequence of the mRNA targets (Fig. 5). Alternatively, Aar base-pairing with its target mRNAs might also stabilize the mRNAs by protecting them from ribonuclease cleavage. This would represent an inconvenient sRNA mechanism, since apart from a few interactions, i.e., DsrA–*rpoS* or GlmZ–*glmS*, sRNA-interference affects more often mRNA destabilisation than activation (Majdalani et al. 1998; Kalamorz et al. 2007).

In contrast to a direct base pair interaction, it is also conceivable that another regulator of amino acid metabolism in *A. baylyi* is involved in the regulation. In fact, we found a putative binding site with 80% identity to the 15-nucleotide *E. coli* Lrp consensus sequence (59 bases downstream of the mapped Aar transcription start site) (Cui et al. 1995). In *E. coli*, Lrp acts as global transcriptional regulator of amino acid metabolism, transport, and pili formation (Newman and Lin 1995). The ADP1 and *E. coli* Lrp proteins contain almost the same size and show 58% sequence identity and 75% sequence similarity regarding the Lrp helix-turn-helix domain. In ADP1, the putative Lrp-binding site in the *aar* gene might indicate negative regulation of the Aar expression by Lrp. We observed that Aar is highly abundant during exponential and stationary growth in complex medium, but only during stationary growth in minimal medium. This agrees with the fact that the *lrp* gene is self-repressed, primarily during growth in complex medium (Lin et al. 1992). During stationary growth in both minimal and complex media, amino acids become scarce and therefore Lrp synthesis might be reduced, which in turn could result in increased Aar levels. An inverse effect is also possible, since *Lrp* was predicted as Aar target (RNAz: −3.768 kcal/mol, interaction site: Fig. 5).

The identification, experimental verification, and initial investigation of a novel and unique sRNA from the soil bacterium *A. baylyi* contribute to the ongoing effort to characterize and understand the extent and function of these exciting new molecules. Obviously, more experimental effort will reveal explanations to the exciting observation of the involvement of Hfq and the direct or indirect connection of Aar to amino acid metabolism.

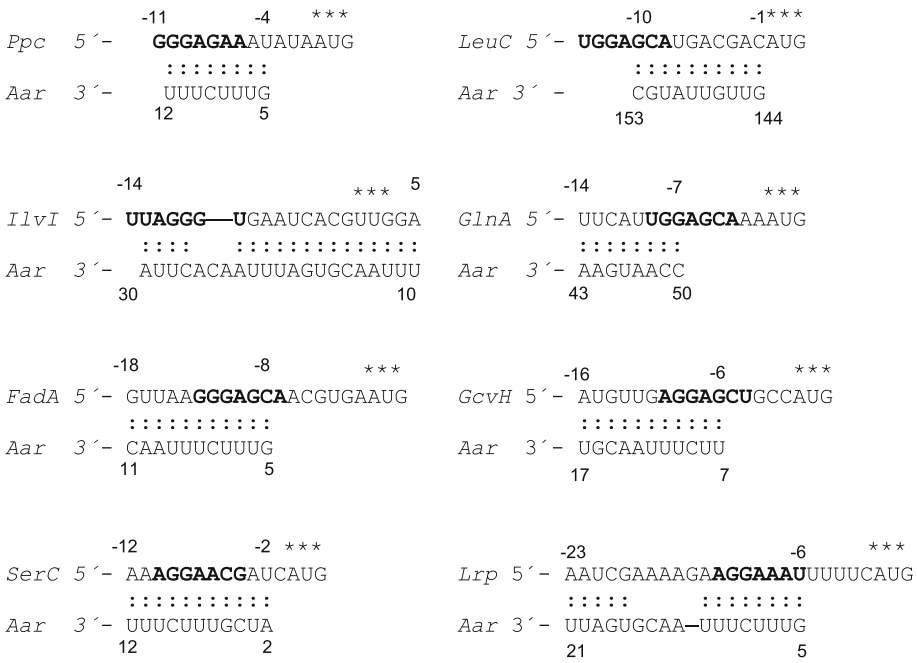

Fig. 5 Predicted interaction sites of Aar and putative mRNA targets. *Letters in bold* indicate the predicted Shine Dalgarno sequences of the corresponding mRNA genes. *Asterisks* mark the start codon of the mRNA, and *numbers* indicate the position of the interaction site within the Aar and mRNA sequences

Experimental procedures

Bacterial strains and growth conditions

Strains of *A. baylyi* (Table 3) were grown in minimal medium with aeration at 30°C as described previously (Trautwein and Gerischer 2001). Carbon sources were used in the following final concentrations: succinate 10 mM, quinate 5 mM, protocatechuate 5 mM, and pyruvate 20 mM. Tetracycline was used as an antibiotic for *A. baylyi* strains containing plasmid pRK415 or its derivates (concentration: 6 μg/μl). Temperature and salt shocks were applied when the corresponding *A. baylyi* culture grown in minimal medium with succinate reached an OD_{600} of about 0.4. After a 30-min incubation, part of the cells was harvested for RNA isolation and the rest was incubated through stationary growth phase. The effect of iron limitation was determined by incubating a culture of ADP1 in minimal medium with succinate under standard iron conditions and then using this culture to inoculate minimal medium with succinate lacking iron sulfate.

E. coli strains were grown in LB medium with aeration at 37°C and were supplied with antibiotics when appropriate (tetracycline 12 μg/μl, ampicillin 100 μg/μl, kanamycin 50 μg/μl).

Plasmid and strain construction

Standard methods were used for plasmid isolation, DNA purification, restriction endonuclease cleavage, ligation, and transformation (Sambrook and Russel 2001). Overexpression of Aar was achieved by cloning *aar* into the broad-host-range plasmid pRK415 (Keen et al. 1988). To obtain the DNA region of interest from the *A. baylyi* genome, a PCR using *Pfu*-DNA polymerase, primers 368/369 (Table 3), and 10 ng *A. baylyi* chromosomal DNA was carried out. The PCR product was gel purified and digested with either *Pst*I/*Hin*dIII or *Pst*I/*Eco*RI. These products were ligated with pRK415 that had been digested with the same enzyme pair, yielding plasmids pRK415 *aar* and pRK415 p*lac aar*, respectively. After transformation into *E. coli* DH5α cells (Hanahan 1983), both plasmids were established via tetracycline resistance. These cloning steps resulted in plasmid pRK415 *aar* expressing Aar from its own promoter and pRK415 p*lac aar* expressing it from the *lac* promoter. P*lac* functions in *A. baylyi* and cannot be controlled using isopropyl *β*-D-1-thiogalactopyranoside, since the bacterium does not have a *lac* operon and the plasmid does not contain *lacI* either. Plasmids were recovered from positive *E. coli* clones and verified by digestion with *Pst*I/*Hin*dIII, *Pst*I/*Eco*RI, and agarose gel electrophoresis. Furthermore, plasmids were sequenced; those without mutations were conjugated by means of plasmid pRK2013 (Figurski and Helinski 1979) from *E. coli* DH5α into *A. baylyi* ADP1. Positive ADP1 clones were selected by growth in minimal medium with 6 μg/μl tetracycline and 5 mM quinate as sole carbon source.

Northern blot analysis

Total RNA was isolated by a previously described procedure (Oelmüller et al. 1990). The RNA quality and concentration were determined by the $OD_{260/280}$ ratio. Fifteen micrograms of purified RNA was combined with RNA loading dye [1 ml

Table 3 Strains, plasmids, and oligonucleotides used in this study

	Relevant characteristics	Source or reference
Strain or plasmid		
ADP1	*Acinetobacter* wild type (strain BD413, ATCC 33305)	Barbe et al. (2004) and Vaneechoutte et al. (2006)
ADP1 pRK415 *aar*	*Acinetobacter* expressing sRNA Aar *in trans* via natural promoter, tet^r	This study
ADP1 pRK415 p*lac aar*	*Acinetobacter* expressing sRNA Aar *in trans* via *lac* promoter, tet^r	This study
ADP1 Δ*hfq*	*Acinetobacter* containing an Ω-interposon instead of *hfq* ORF, spe^r	Schilling and Gerischer (2009)
ADP1 pRK415 *hfq*	*Acinetobacter* expressing Hfq *in trans* via natural promoter, tet^r	Schilling and Gerischer (2009)
DH5α	*Escherichia coli* general cloning strain	Hanahan (1983)
pBSKII+	ColE1 replicon, amp^r, *lacZα*, 2,958 bp	Stratagene
pRK415	RK2 replicon, tet^r, 10,500 bp	Keen et al. (1988)
pRK2013	ColE1 replicon, kan^r, 4,800 bp	Figurski and Helinski (1979)
pRK415 *aar*	*aar* region (2,812,113–2,812,606) cloned with *Eco*RI/*Pst*I in pRK415	This study
pRK415 *aar Plac*	*aar* region (2,812,113–2,812,606) cloned with *Hin*dIII/*Pst*I in pRK415	This study
Oligonucleotide/sequence 5′–3′		
315/CTAGTGGAGACCCCTAAGGTTTG	368/GGA**GAATTCAAGCTT**CTGGACGAAGTAAAAGAAGG	419/TGAGCATGGCGAACAAGGTC
316/GGTATTACGCCTTATGGTGTGTTT	369/GGA**CTGCAG**CGTGCTGGCATGGCATATAC	420/ACCGCCTTTAACACGTGGAC
331/GCGTAACGATTGGGGTGATC	396/AATGCTCGTTCGCGCACTCG	421/TGTTGCAGCAAGCCGTGAAG
332/CACTTATTAACGTGAATACCAATGAA	397/TCGCTTGCATGGCGGACTTG	422/CTTCGCTACGGCGAAACAGG
336/TATTCTCTAGTGAGGTCGGC	398/ATGCTGGGTCGTATGAATGG	423/CTTGCAGGTCGTCAGCCTTG
337/AGAAGGAGCGAACATTCGCC	399/TTTCTGCGTTGCTGGAACTG	424/CCAATGATCGCCAATACCAC
345/AGT**CTCGAG**TTGGGGGAGTGCATAACCTATTCCG	356/AGT**CTGCAG**GTGAATACAGATTCGTTGTTATGCG	425/GCGTGCGTACAATTTCTGTG
346/AGT**CTGCAG**AACATTCTACTTTACCGAAGCTGTG	402/GCAAGGTCCACCACCCAATC	426/GAACATAAGCGGCATCTTGG
347/AGT**CTCGAG**TAAACACACCATAAGGCGATTTACC	403/CATCACGGTCACCACCCATC	431/AGATGCCTTAGGCGATCTTG
348/AGT**CTGCAG**GCAATGTCTGGTGTGTGGCACTAGG	404/AAGCCTTCGAGCGCCCAAAC	432/GATCTACGTCTGCGATGTTG
355/AGT**CTCGAG**TAGGGTAACACTCATTGTTCATTGG	405/CATCCACACCGCGTACATAG	377/TCACAGCTTCGGTAAAGTAG
		378/GGGAGTGCATAACTTATTCC

Bold letters indicate recognition sites of restriction enzymes (*Xho*I, *Pst*I, *Eco*RI, *Hin*dIII)

5× RNA loading dye = 8 µl 500 mM ethylenediaminetetraacetic acid, 200 µl 100% glycerol, 72 µl 37% formaldehyde, 308 µl formamide, 400 µl 10× running buffer (200 mM 3-(*N*-morpholino)propanesulfonic acid, 50 mM sodium acetate, 5 mM ethylenediaminetetraacetic acid, pH 7), 2 µl saturated bromphenol blue, 10 µl deionized water] and then heat-denatured for 5 min at 65°C. Afterward, RNA was separated on a 1.2% formaldehyde–agarose gel and transferred to a Hybond-N+ nylon membrane by capillary blotting overnight with 10× SSC [1.5 M sodium chloride, 0.15 mM tri-sodium citrate]. The membrane was dried at 25°C, and the RNA was covalently bound to the membrane by UV cross-linking for 90 s at 120,000 µJ/cm^2. Specific RNA detection was performed by the DIG labeling and detection system (Roche Applied Science, Mannheim, Germany) with specific PCR probes and primers 315/316 (sRNA2), 331/332 (Aar), 396/397 (*IlvI*), 398/399 (*FadA*), 402/403 (*Ppc*), 404/405 (*MinE*), 419/420 (*GlnA*), 421/422 (*GlnT*), 423/424 (*LeuC*), 425/426 (*SerC*), and 431/432 (*GcvH*) (Table 3).

RNA end mapping

RNA ends were mapped by a modified protocol of the circularized RT-PCR method described previously (Forner et al. 2007). Here, 5 µg of RNA (treated with 25 U tobacco acid pyrophosphatase for 1 h at 37°C) was denatured at 65°C for 10 min and quickly cooled on ice. RNA self-ligation was performed with 40 U T4 RNA ligase I, 10 U RNase inhibitor, 1 U RNase-free DNase I, and 1× T4 RNA ligase buffer (50 mM Tris, 10 mM magnesium chloride, 1 mM adenosine triphosphate, 10 mM dithiothreitol, pH 7.8) in a total volume of 25 µl at 37°C for 2 h. The volume was adjusted with water to 500 µl, and the enzymes were removed by phenol treatment. Self-ligated RNA was precipitated overnight at −20°C with 250 mM sodium acetate pH 5.2 and 100% ethanol. Finally, cDNA synthesis was performed with 0.5 mM dNTP's, 1 pmol gene-specific primer, 355 for Aar and 347 for sRNA2 (Table 3), 5 µg self-ligated RNA, 200 U reverse transcriptase (RNase H minus mutant) in 1× RT buffer (50 mM Tris, 75 mM potassium chloride, 3 mM magnesium chloride, 10 mM dithiothreitol, pH 8.3) for 2 h at 45°C. PCR was carried out with 2.5 µl of heat-treated cDNA reaction (70°C, 10 min) and primers 355/346 (Aar), 347/348 (sRNA2), in a standard PCR mixture. Alternatively, 5′-RACE experiments (Roche Applied Science, Mannheim, Germany) were performed for *aar* as described in the manual with primer 377 and nested primer 378 (Table 3).

PCR

Primer sequences (Table 3) were selected to have a melting temperature of at least 60°C. The PCR conditions including *Taq*- or *Pfu*-DNA polymerase were 95°C for 5 min, followed by 30 cycles of denaturation at 95°C for 45 s, annealing at 54°C for 1 min, and extension at 72°C for at least 30 s (longer for products over 500 bases in length).

sRNA gene and mRNA target predictions

Comparative intergenic genome analysis of *A. baylyi* ADP1 (NCBI Refseq Id NC_005966) and *A. baumannii* ATCC17978 (NCBI Refseq Id NC_009085) in combination with the detection of thermodynamically stable putative non-coding RNAs using RNAz (Washietl et al. 2005) was kindly performed by Voss et al. (2009). This initial computer-aided search resulted in 481 non-coding RNA candidates. Inspection of these predicted loci revealed among others Aar, with a *Z*-score of −3.09 and a *P*-value of 0.99, to be a good candidate for further analysis.

Putative mRNA targets of Aar were predicted by two bioinformatic programs: IntaRNA (Busch et al. 2008) and RNAup (Mückstein et al. 2006). Both programs utilize a model based on the hybridization energy of the two interacting RNAs as well as the energy required to make the interaction sites in both molecules accessible (based on all possible conformations). The main difference between the two programs is that IntaRNA enforces a region of continuous pairing (seed region) as a hybridization start. Here, a minimum seed length of eight base pairs was required. The search for interactions was performed in a region of 250 nt upstream and 150 nt downstream of each *A. baylyi* annotated mRNA. As part of the IntaRNA prediction algorithm, only interactions that involve the highly conserved regions of Aar (positions 10–53 and 136–149) RNA were considered. The most predominant mechanism of post-transcriptional gene regulation by *trans*-encoded sRNAs is interference with ribosome binding to the Shine Dalgarno (SD) sequence followed by degradation of the mRNA–sRNA duplex. Therefore, SD sequence locations for all mRNAs were predicted by simulating hybridization with the single-stranded 3′-tail of the 16S rRNA (Starmer et al. 2006). Targets for which Aar RNA was predicted to bind at or in the immediate vicinity of the SD sequence were selected for further analysis. Additional targets were predicted by RNAup and a pipeline based on sequence as well as interaction site conservation of both molecules. Using a reciprocal best BLAST approach (http://www.bioinf.uni-leipzig.de/Software/proteinOrtho/), all annotated protein coding genes of *A. baylyi* orthologs within the six completely sequenced and annotated *A. baumanni* strains (NCBI Refseq Ids NC_010611, NC_011586, NC_009085 NC_010410, NC_011595 and NC_010400) were identified. Then, optimal interactions for each Aar homolog were predicted in the corresponding species. Only interactions conserved in at least five *Acinetobacter* strains were assumed to be functional.

Acknowledgments We would like to thank Björn Voss for his predictions of sRNA genes in *Acinetobacter* and Véronique de Berardinis for her effort to delete *aar*. Furthermore, we would like to thank Iris Steiner for her contribution. This work was supported by the German Federal Ministry of Education and Research (BMBF grant 0313921 FRISYS to A.S.R.); the German Research Foundation (DFG grant SPP1258 to S.F. STA850/7-1 and A.S.R. BA2168/2-1); and the state of Baden-Württemberg, Germany (personal LGFG grant to D.S.).

References

Altuvia S (2007) Identification of bacterial small non-coding RNAs: experimental approaches. Curr Opin Microbiol 10:257–261

Argaman L, Hershberg R, Vogel J, Bejerano G, Wagner EG, Margalit H, Altuvia S (2001) Novel small RNA-encoding genes in the intergenic regions of *Escherichia coli*. Curr Biol 11:941–950

Axmann IM, Kensche P, Vogel J, Kohl S, Herzel H, Hess WR (2005) Identification of cyanobacterial non-coding RNAs by comparative genome analysis. Genome Biol 6:R73

Barbe V, Vallenet D, Fonknechten N, Kreimeyer A, Oztas S, Labarre L, Cruveiller S, Robert C, Duprat S, Wincker P, Ornston LN, Weissenbach J, Marliere P, Cohen GN, Medigue C (2004) Unique features revealed by the genome sequence of *Acinetobacter* sp. ADP1, a versatile and naturally transformation competent bacterium. Nucleic Acids Res 32:5766–5779

Bejerano-Sagie M, Xavier KB (2007) The role of small RNAs in quorum sensing. Curr Opin Microbiol 10:189–198

Boisset S, Geissmann T, Huntzinger E, Fechter P, Bendridi N, Possedko M, Chevalier C, Helfer AC, Benito Y, Jacquier A, Gaspin C, Vandenesch F, Romby P (2007) *Staphylococcus aureus* RNAIII coordinately represses the synthesis of virulence factors and the transcription regulator Rot by an antisense mechanism. Genes Dev 21:1353–1366

Brescia CC, Mikulecky PJ, Feig AL, Sledjeski DD (2003) Identification of the Hfq-binding site on DsrA RNA: Hfq binds without altering DsrA secondary structure. Rna 9:33–43

Buck D, Guest JR (1989) Overexpression and site-directed mutagenesis of the succinyl-CoA synthetase of *Escherichia coli* and nucleotide sequence of a gene (*g30*) that is adjacent to the *suc* operon. Biochem J 260:737–747

Busch A, Richter AS, Backofen R (2008) IntaRNA: efficient prediction of bacterial sRNA targets incorporating target site accessibility and seed regions. Bioinformatics 24:2849–2856

Calvo JM, Matthews RG (1994) The leucine-responsive regulatory protein, a global regulator of metabolism in *Escherichia coli*. Microbiol Rev 58:466–490

Cui Y, Wang Q, Stormo GD, Calvo JM (1995) A consensus sequence for binding of Lrp to DNA. J Bacteriol 177:4872–4880

de Berardinis V, Vallenet D, Castelli V, Besnard M, Pinet A, Cruaud C, Samair S, Lechaplais C, Gyapay G, Richez C, Durot M, Kreimeyer A, Le Fevre F, Schachter V, Pezo V, Doring V, Scarpelli C, Medigue C, Cohen GN, Marliere P, Salanoubat M, Weissenbach J (2008) A complete collection of single-gene deletion mutants of *Acinetobacter baylyi* ADP1. Mol Syst Biol 4:174

de Boer PA, Crossley RE, Rothfield LI (1989) A division inhibitor and a topological specificity factor coded for by the minicell locus determine proper placement of the division septum in *E. coli*. Cell 56:641–649

Delihas N, Forst S (2001) MicF: an antisense RNA gene involved in response of *Escherichia coli* to global stress factors. J Mol Biol 313:1–12

Figurski DH, Helinski DR (1979) Replication of an origin-containing derivative of plasmid RK2 dependent on a plasmid function provided *in trans*. Proc Natl Acad Sci USA 76:1648–1652

Folichon M, Allemand F, Regnier P, Hajnsdorf E (2005) Stimulation of poly(A) synthesis by *Escherichia coli* poly(A)polymerase I is correlated with Hfq binding to poly(A) tails. FEBS J 272:454–463

Forner J, Weber B, Thuss S, Wildum S, Binder S (2007) Mapping of mitochondrial mRNA termini in *Arabidopsis thaliana*: t-elements contribute to 5′ and 3′ end formation. Nucleic Acids Res 35:3676–3692

Gardner PP, Daub J, Tate JG, Nawrocki EP, Kolbe DL, Lindgreen S, Wilkinson AC, Finn RD, Griffiths-Jones S, Eddy SR, Bateman A (2009) Rfam: updates to the RNA families database. Nucleic Acids Res 37:D136–D140

Geissmann TA, Touati D (2004) Hfq, a new chaperoning role: binding to messenger RNA determines access for small RNA regulator. EMBO J 23:396–405

Gorke B, Vogel J (2008) Non-coding RNA control of the making and breaking of sugars. Genes Dev 22:2914–2925

Gottesman S (2005) Micros for microbes: non-coding regulatory RNAs in bacteria. Trends Genet 21:399–404

Hajnsdorf E, Regnier P (2000) Host factor Hfq of *Escherichia coli* stimulates elongation of poly(A) tails by poly(A) polymerase I. Proc Natl Acad Sci USA 97:1501–1505

Hanahan D (1983) Studies on transformation of *Escherichia coli* with plasmids. J Mol Biol 166:557–580

Hershberg R, Altuvia S, Margalit H (2003) A survey of small RNA-encoding genes in *Escherichia coli*. Nucleic Acids Res 31:1813–1820

Kalamorz F, Reichenbach B, Marz W, Rak B, Gorke B (2007) Feedback control of glucosamine-6-phosphate synthase GlmS expression depends on the small RNA GlmZ and involves the novel protein YhbJ in *Escherichia coli*. Mol Microbiol 65:1518–1533

Kawamoto H, Koide Y, Morita T, Aiba H (2006) Base-pairing requirement for RNA silencing by a bacterial small RNA and acceleration of duplex formation by Hfq. Mol Microbiol 61:1013–1022

Kawano M, Reynolds AA, Miranda-Rios J, Storz G (2005) Detection of 5′- and 3′-UTR-derived small RNAs and cis-encoded antisense RNAs in *Escherichia coli*. Nucleic Acids Res 33:1040–1050

Keen NT, Tamaki S, Kobayashi D, Trollinger D (1988) Improved broad-host-range plasmids for DNA cloning in Gram-negative bacteria. Gene 70:191–197

Kingsford CL, Ayanbule K, Salzberg SL (2007) Rapid, accurate, computational discovery of Rho-independent transcription terminators illuminates their relationship to DNA uptake. Genome Biol 8:R22

Le Derout J, Folichon M, Briani F, Deho G, Regnier P, Hajnsdorf E (2003) Hfq affects the length and the frequency of short oligo(A) tails at the 3′ end of *Escherichia coli* rpsO mRNAs. Nucleic Acids Res 31:4017–4023

Le Derout J, Boni IV, Regnier P, Hajnsdorf E (2010) Hfq affects mRNA levels independently of degradation. BMC Mol Biol 11:17

Lin R, D'Ari R, Newman EB (1992) Lambda p*lac*Mu insertions in genes of the leucine regulon: extension of the regulon to genes not regulated by leucine. J Bacteriol 174:1948–1955

Liu MY, Gui G, Wei B, Preston JF 3rd, Oakford L, Yuksel U, Giedroc DP, Romeo T (1997) The RNA molecule CsrB binds to the global regulatory protein CsrA and antagonizes its activity in *Escherichia coli*. J Biol Chem 272:17502–17510

Livny J, Waldor MK (2007) Identification of small RNAs in diverse bacterial species. Curr Opin Microbiol 10:96–101

Livny J, Brencic A, Lory S, Waldor MK (2006) Identification of 17 *Pseudomonas aeruginosa* sRNAs and prediction of sRNA-encoding genes in 10 diverse pathogens using the bioinformatic tool sRNAPredict2. Nucleic Acids Res 34:3484–3493

Majdalani N, Cunning C, Sledjeski D, Elliott T, Gottesman S (1998) DsrA RNA regulates translation of RpoS message by an anti-antisense mechanism, independent of its action as an antisilencer of transcription. Proc Natl Acad Sci USA 95:12462–12467

Maki K, Uno K, Morita T, Aiba H (2008) RNA, but not protein partners, is directly responsible for translational silencing by a bacterial Hfq-binding small RNA. Proc Natl Acad Sci USA 105:10332–10337

Masse E, Gottesman S (2002) A small RNA regulates the expression of genes involved in iron metabolism in *Escherichia coli*. Proc Natl Acad Sci USA 99:4620–4625

Masse E, Escorcia FE, Gottesman S (2003) Coupled degradation of a small regulatory RNA and its mRNA targets in *Escherichia coli*. Genes Dev 17:2374–2383

Masse E, Salvail H, Desnoyers G, Arguin M (2007) Small RNAs controlling iron metabolism. Curr Opin Microbiol 10:140–145

Mizuno T, Chou MY, Inouye M (1984) A unique mechanism regulating gene expression: translational inhibition by a complementary RNA transcript (micRNA). Proc Natl Acad Sci USA 81:1966–1970

Moll I, Afonyushkin T, Vytvytska O, Kaberdin VR, Blasi U (2003) Coincident Hfq binding and RNase E cleavage sites on mRNA and small regulatory RNAs. Rna 9:1308–1314

Mückstein U, Tafer H, Hackermuller J, Bernhart SH, Stadler PF, Hofacker IL (2006) Thermodynamics of RNA-RNA binding. Bioinformatics 22:1177–1182

Munch R, Hiller K, Barg H, Heldt D, Linz S, Wingender E, Jahn D (2003) PRODORIC: prokaryotic database of gene regulation. Nucleic Acids Res 31:266–269

Newman EB, Lin R (1995) Leucine-responsive regulatory protein: a global regulator of gene expression in *E. coli*. Annu Rev Microbiol 49:747–775

Oelmüller U, Krüger N, Steinbüchel A, Freidrich CG (1990) Isolation of prokaryotic RNA and detection of specific mRNA with biotinylated probes. J Microbiol Methods 11:73–81

Pfeiffer V, Sittka A, Tomer R, Tedin K, Brinkmann V, Vogel J (2007) A small non-coding RNA of the invasion gene island (SPI-1) represses outer membrane protein synthesis from the *Salmonella* core genome. Mol Microbiol 66:1174–1191

Regnier P, Hajnsdorf E (2008) The role of RNA chaperone Hfq in poly(A) metabolism methods to determine positions, abundance, and lengths of short oligo(A) tails. Methods Enzymol 447:161–181

Sambrook J, Russel DW (2001) Molecular cloning: a laboratory manual, 3rd edn. Cold Spring Harbor Laboratory Press, Cold Spring Harbor

Schilling D, Gerischer U (2009) The *Acinetobacter baylyi hfq* gene encodes a large protein with an unusual C terminus. J Bacteriol 191:5553–5562

Schimmel PR, Soll D (1979) Aminoacyl-tRNA synthetases: general features and recognition of transfer RNAs. Annu Rev Biochem 48:601–648

Sharma CM, Darfeuille F, Plantinga TH, Vogel J (2007) A small RNA regulates multiple ABC transporter mRNAs by targeting C/A-rich elements inside and upstream of ribosome-binding sites. Genes Dev 21:2804–2817

Sonnleitner E, Sorger-Domenigg T, Madej MJ, Findeiss S, Hackermuller J, Huttenhofer A, Stadler PF, Blasi U, Moll I (2008) Detection of small RNAs in *Pseudomonas aeruginosa* by RNomics and structure-based bioinformatic tools. Microbiology 154:3175–3187

Soper TJ, Woodson SA (2008) The *rpoS* mRNA leader recruits Hfq to facilitate annealing with DsrA sRNA. Rna 14:1907–1917

Starmer J, Stomp A, Vouk M, Bitzer D (2006) Predicting Shine-Dalgarno sequence locations exposes genome annotation errors. PLoS Comput Biol 2:e57

Trautwein G, Gerischer U (2001) Effects exerted by transcriptional regulator PcaU from *Acinetobacter* sp. strain ADP1. J Bacteriol 183:873–881

Tu KC, Bassler BL (2007) Multiple small RNAs act additively to integrate sensory information and control quorum sensing in *Vibrio harveyi*. Genes Dev 21:221–233

Udekwu KI, Darfeuille F, Vogel J, Reimegard J, Holmqvist E, Wagner EG (2005) Hfq-dependent regulation of OmpA synthesis is mediated by an antisense RNA. Genes Dev 19:2355–2366

Valentin-Hansen P, Eriksen M, Udesen C (2004) The bacterial Sm-like protein Hfq: a key player in RNA transactions. Mol Microbiol 51:1525–1533

Vanderpool CK (2007) Physiological consequences of small RNA-mediated regulation of glucose-phosphate stress. Curr Opin Microbiol 10:146–151

Vaneechoutte M, Young DM, Ornston LN, De Baere T, Nemec A, Van Der Reijden T, Carr E, Tjernberg I, Dijkshoorn L (2006) Naturally transformable *Acinetobacter* sp. strain ADP1 belongs to the newly described species *Acinetobacter baylyi*. Appl Environ Microbiol 72:932–936

Vogel J, Papenfort K (2006) Small non-coding RNAs and the bacterial outer membrane. Curr Opin Microbiol 9:605–611

Voss B, Georg J, Schon V, Ude S, Hess WR (2009) Biocomputational prediction of non-coding RNAs in model cyanobacteria. BMC Genomics 10:123

Washietl S, Hofacker IL, Stadler PF (2005) Fast and reliable prediction of non-coding RNAs. Proc Natl Acad Sci USA 102:2454–2459

Wassarman KM (2007) 6S RNA: a small RNA regulator of transcription. Curr Opin Microbiol 10:164–168

Willkomm DK, Minnerup J, Hüttenhofer A, Hartmann RK (2005) Experimental RNomics in *Aquifex aeolicus*: identification of small non-coding RNAs and the putative 6S RNA homolog. Nucleic Acids Res 33:1949–1960